Advances in Water Resources 193 (2024) 104823

Contents lists available at ScienceDirect

Advances in Water Resources

journal homepage: www.elsevier.com/locate/advwatres

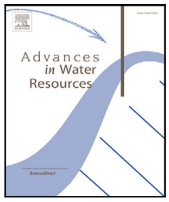

A simple and robust approach for adapting design storms to assess climate-induced changes in flash flood hazard

Nadav Peleg [a,1], Daniel B. Wright [b], Hayley J. Fowler [c], João P. Leitão [d], Ashish Sharma [e], Francesco Marra [f,*,1]

[a] Institute of Earth Surface Dynamics, University of Lausanne, 1015 Lausanne, Switzerland
[b] Department of Civil and Environmental Engineering, University of Wisconsin-Madison, Madison, WI 53706, USA
[c] School of Engineering, Newcastle University, Newcastle upon Tyne NE1 7RU, UK
[d] Department of Urban Water Management, Swiss Federal Institute of Aquatic Science and Technology, 8600 Dubendorf, Switzerland
[e] School of Civil and Environmental Engineering, University of New South Wales, Sydney, NSW 2052, Australia
[f] Department of Geosciences, University of Padova, 35131 Padua, Italy

ARTICLE INFO

Keywords:
Extreme precipitation
Rainfall return level
Present and future IDF curves
Design storm implementation

ABSTRACT

Hydrologists and civil engineers often use design storms to assess flash flood hazards in urban, rural, and mountainous catchments. These synthetic storms are not representations of real extreme rainfall events, but rather simplified versions parameterized to mimic extreme precipitation statistics often obtained from intensity–duration–frequency (IDF) curves. To construct design storms for the future climate, it is thus necessary first to recalculate IDF curves to represent rainfall under warmer conditions. We propose a framework for adjusting IDF curves and design storms to future climate conditions using the TENAX model, a novel statistical approach that can provide future short-duration precipitation return levels based on projected temperature changes. For most applications, information from climate models at the daily scale can be used to construct design storms at the sub-hourly scale without any downscaling or bias adjustment. Our approach is illustrated through a re-parameterization of the Chicago Design Storm (CDS) in the context of climate change. As a case study demonstration, we apply the TENAX model to data from the city of Zurich to calculate changes in the historical IDF curve for durations ranging from 10 min to 3 h. We then construct synthetic 100-year return period design storms based on the CDS for present and future climates and use the CAFlood model to produce flood inundation maps to assess changes in flood hazard. The codes for adapting design storms to climate change are simple to implement, easily applicable by practitioners, and made freely available.

1. Introduction

Extreme rainfall events with short duration are the main cause of pluvial and flash floods and recent years have shown that climate change has increased the frequency and magnitude of these events (Kundzewicz et al., 2014). The Clausius–Clapeyron relation partially explains this trend, which relates rising air temperatures with an increase in atmospheric water capacity, resulting in the intensification of rainfall (Trenberth et al., 2003). Hence, continued warming will result in further intensification of extreme rainfall (Min et al., 2011); particularly short-duration convective rainfall (Prein et al., 2017; Fowler et al., 2021). This will likely result in more frequent and more severe flash floods in urban (Rosenzweig et al., 2018), rural (Yin et al., 2018), and mountainous (Borga et al., 2014) areas, leading to increased fatalities and infrastructure damage. The development of effective adaptation strategies requires a thorough assessment of the impact of climate change on flash floods.

Many methods have been proposed for assessing extreme rainfall and flood changes in a future climate (for an overview see: Willems et al. (2012), Arnbjerg-Nielsen et al. (2013), Madsen et al. (2014) and Maimone et al. (2023)). Some specific examples include: (i) incorporating rainfall data directly from climate models into hydrological models (often with some sort of bias correction; Smith et al. (2014)); (ii) obtaining extreme rainfall events from an observed archive and intensifying them by a factor derived from climate models (also known as the change factor approach; Fatichi et al. (2011)) or by estimating

* Corresponding author.
E-mail addresses: nadav.peleg@unil.ch (N. Peleg), francesco.marra@unipd.it (F. Marra).
[1] Contributed equally to this manuscript.

https://doi.org/10.1016/j.advwatres.2024.104823
Received 23 February 2024; Received in revised form 27 August 2024; Accepted 12 September 2024
Available online 17 September 2024

a relationship with a climate variable (frequently near-surface air temperature is used; Peleg et al. (2022)); (iii) simulating extreme storms for present and future periods using a stochastic rainfall generator model (Kilsby et al., 2007; Peleg et al., 2017, 2019; Moraga et al., 2021) or using a stochastic storm transposition model to resample observed storm events to generate hypothetical extreme storms for the future (Yu et al., 2020; Wright et al., 2020); and (iv) utilizing an analog approach, in which extreme storms recorded in one location are projected to another location which matches the climate conditions of that location in the future (Wang et al., 2019). These methods are all scientifically sound but rely on strong assumptions (e.g., quantitative accuracy of model simulations, no changes in atmospheric dynamics) and they are often computationally intensive.

Alternatively, extreme storms can be parameterized and represented with design storms. These are simplified versions of extreme storms that can be used to simulate the hydrological responses to unseen but possible precipitation events using a rainfall-runoff model (Marsalek and Watt, 1984; Watt and Marsalek, 2013). This approach is computationally much faster and less complex than the methods described above, as an extreme storm for a given return level (e.g., an event that occurs on average every ten years) can be simulated via a single synthetic storm. Despite its simplicity, this method provides valuable flood hazard information, since design storms and their resulting design flow response may be tailored to specific return levels of interest (Keifer and Chu, 1957; Rosbjerg and Madsen, 2019). Design storms are commonly used in urban drainage system planning (Markolf et al., 2021), as well as in estimating the risks and damages associated with flash floods in rural catchments (Berk et al., 2017).

Design storms are not a new concept (Watt and Marsalek, 2013; Markolf et al., 2021). Our first knowledge of design storms dates back over 130 years to the groundbreaking research of Kuichling (1889). The approach gained popularity and was further developed by researchers and practitioners from the 1930s onward (for example, refer to Hicks (1944), Keifer and Chu (1957) and Tholin and Keifer (1960)). Various types of design storm exist today (for a few examples, see Balbastre-Soldevila et al. (2019)). Among them, the Chicago Design Storm (CDS; Keifer and Chu (1957)) and variations thereof, such as the Alternating Block Method (Chow et al., 1988), yield hyetographs that are constructed in such a way that they simulate extreme rainfall in accordance with rainfall intensities sampled directly from intensity–duration–frequency (IDF) curves, as described further in Section 2.2.

When using the design storm approach to assess the impact of climate change on floods, it is necessary to compute IDF curves for current and future climates (Schlef et al., 2023). Common practice is to compute IDF curves based on a long time series of observed precipitation data and to then re-compute these for a future climate by applying a statistical transformation of the observed time series (e.g., using the quantile mapping approach; Rajulapati and Papalexiou (2023)) based on data from climate models. Other methods can be used to alter a historical time series of precipitation to represent future conditions (as presented by Dinh and Aires (2023)). These approaches (and others, see review by Martel et al. (2021)) require interpretation of climate model simulations of precipitation. This may lead to increased uncertainty in the projections of future IDF curves and design storms owing to three factors: (i) many design storms are required to be at sub-hourly scales due to the rapid hydrological response time of urban floods (Ochoa-Rodriguez et al., 2015) and rural flash floods (Borga et al., 2014). Despite this, most climate model data are only available at a coarser time resolution (often daily or, at most, hourly), and the transformation from observed to future time series is therefore based on the assumption that the factor of change derived from the daily or hourly time-scale can also be applied to the sub-hourly time-scale (Bordoy and Burlando, 2014). While Blanchet et al. (2016) suggested a parameterization to scale down IDF curves (GEV-based) to the hourly resolution (further developed by Lima et al. (2018)), it has not been explored at the sub-hourly scale. Innocenti et al. (2017) presented a simple GEV-based scaling method that was successfully validated at sub-hourly scales, but noted that with climate change the scaling might not be effective, as extreme rainfall on a sub-hourly basis will likely respond to global warming with different sensitivity to temperature than those expected on a daily basis; (ii) climate models cannot explicitly resolve convective processes (Prein et al., 2015), unless convection-permitting models are employed, making it virtually impossible to adequately represent changes in sub-daily convective extreme rainfall intensities; and (iii) since the procedure consists of three steps (i.e., shifting the observed rainfall time series, fitting the parameters for the IDF curve, and fitting the parameters for the design storm), uncertainty is accumulated and propagated from each step to the next (Cook et al., 2020).

Marra et al. (2024) recently proposed a physics-based statistical model called TENAX that can assess changes in IDF curves for short-duration precipitation extremes (these are mostly generated by convective processes and the most conducive to the production of flash floods) with temperature without the need to simulate or adjust the precipitation time series. The TENAX model requires only three parameters for climate adjustment of IDF estimates: the change in the average and standard deviation of air temperature during rainy days, and the change in the annual number of precipitation events. These can all be obtained from coarse-resolution climate models at a daily scale, by analyzing the temperature time series for the days on which precipitation was recorded. This directly addresses point (i) above and reduces the level of uncertainty in design storm and flood hazard assessment by removing the need for the first step in point (iii) also mentioned above.

Here, we present the further development of the TENAX model to compute design storms in the context of climate change, integrating the CDS approach into the model. The codes are open-source and have been made available for other hydrologists and practitioners to use. We demonstrate our methodology for the city of Zurich in Switzerland and briefly discuss the TENAX-CDS model's limitations and advantages.

2. Methods

An overview of the proposed approach to estimating changes in IDF curves, design storms, and flood responses as a result of climate change is shown in Fig. 1. Data input requirements for TENAX-CDS are minimal: (i) observed time series of precipitation (P_p, with a minimum temporal resolution equal to that required for the IDF) and temperature (T_p, minimum temporal resolution is daily) representing the present climate, and (ii) information on the change of mean and standard deviation of temperature during wet days ($\Delta T = T_f - T_p$ and $\frac{\sigma_f}{\sigma_p}$, respectively; where $_p$ and $_f$ subscript indicate present and future estimates), and on the change in the total annual number of rainfall events ($\frac{n_f}{n_p}$) as derived from daily climate model projections. The TENAX-CDS model code (Peleg and Marra, 2024) is open-source; details are provided in the "code availability" section.

In the following subsections, we briefly present the TENAX (Section 2.1) and CDS (Section 2.2) models; later we present the CAFlood model (Section 2.3) that was used to translate the present and future CDSs into inundation maps in our case study.

2.1. The TENAX model

The TENAX model (Marra et al., 2024) is an abbreviation for "TEmperature-dependent Non-Asymptotic statistical model for eXtreme return levels". Below, a concise description of the model is presented. Readers are referred to Marra et al. (2024) for further details.

The TENAX model separates the dependence of extreme precipitation on temperature (i.e., the physics of short-duration precipitation extremes at a given temperature) from the occurrence of precipitation

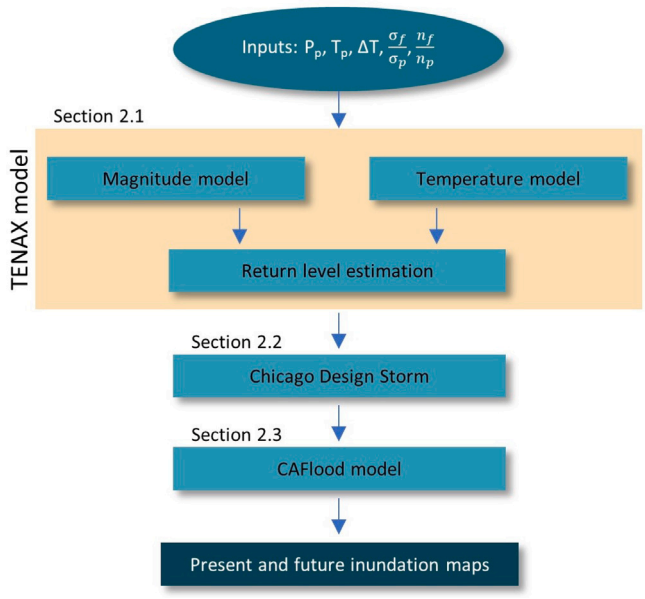

Fig. 1. A flowchart of the TENAX-CDS approach for assessing flood inundation changes due to climate change.

events at a given temperature, and combines this information to derive precipitation return levels. TENAX is based on a non-asymptotic statistical methodology, which models duration maxima of independent storms instead of block maxima (typically annual maxima). This approach allows one to reconcile the approaches based on the extreme precipitation–temperature scaling relation with a sound estimation of extreme precipitation return levels with low frequency. Three components are combined to achieve this (Fig. 1): (i) a "magnitude component" — a non-stationary statistical model for the cumulative distribution function of the magnitude of precipitation events, incorporating temperature as a covariate; (ii) a "temperature component" — a function describing the probability density of temperatures during precipitation events; and (iii) a "return level estimation component" — a non-asymptotic formulation for extreme precipitation return levels.

(i) Magnitude component. Precipitation magnitudes x for a duration t_D of interest are defined as the maximum intensities at the duration t_D observed during independent storms. Details on the identification of independent storms are given in Marra et al. (2020). The Weibull distribution is used to model precipitation magnitudes (x). The Weibull parameters (scale and shape) are made explicitly dependent on near-surface air temperature (T):

$$W(x;T) = 1 - \mathrm{e}^{-\left[\frac{x}{\lambda_0 \cdot \mathrm{e}^{aT}}\right]^{\kappa_0 + bT}}, \tag{1}$$

where λ_0 and a describe the dependence of the scale parameter on temperature, which is exponential, as supported by theory and by numerous studies (e.g., see Fowler et al. (2021)), and κ_0 and b describe the dependence (if any) of the shape parameter on temperature via a simple linear relation. Note that previous applications by the authors found that b is not significantly different from 0.

(ii) Temperature component. A Generalized Gaussian distribution can be used to model the temperature associated with precipitation events (i.e., the average temperature during the 24 h leading up to the event peak intensity). Its probability density function is:

$$g(T) = \frac{2}{\sigma \cdot \Gamma(1/4)} \cdot \exp\left[-\left(\frac{T-\mu}{\sigma}\right)^4\right], \tag{2}$$

where μ is the location and σ is the scale parameters. It is important to note here that different regions may require different descriptions of the temperature distribution. For example, the authors found that for some applications focusing only on summer months, a normal distribution can be used (see also Marra et al., 2024).

(iii) Return level estimation component. Non-asymptotic extreme value statistics (Marani and Ignaccolo, 2015) builds on the consideration that when the marginal cumulative distribution function $F(x)$ describing all the independent realizations of the process of interest is known (which can be tested, e.g., see Marra et al. (2023)), the cumulative distribution function $G(x)$ of annual maxima emerging from a finite number n of independent events per year sampled from $F(x)$ can be written as:

$$G(x) = F(x)^n. \tag{3}$$

Once the magnitude $W(x;T)$ and the temperature $g(T)$ components are established, a stochastic approach can be used to generate a large collection of temperatures T_i with $i = 1, \ldots, N$ sampled from $g(T)$ to obtain a Monte Carlo approximation of $F(x)$. An estimate of the distribution of annual maxima can then be obtained using the Simplified Metastatistical Extreme Value formulation (SMEV) formulation (Marra et al., 2019):

$$G_{\mathrm{TENAX}}(x) = \left(\int_{-\infty}^{\infty} W(x;T) \cdot g(T) dT\right)^n \simeq \left(\frac{1}{N}\sum_{i=1}^{N} W(x;T_i)\right)^n, \tag{4}$$

where N is the number of stochastically-generated events and n is the average number of independent events in a year. Precipitation return levels can be then computed by the inversion of Eq. (4).

Model uncertainty is computed by fitting the parameters of the model multiple times (here, 500 iterations were applied) by bootstrapping the observed precipitation and temperature data (bootstrapping with replacement of years in the record, as in Marra et al. (2024)). Estimation uncertainties computed by the TENAX model are reduced compared to those obtained by employing GEV-based methods (Marra et al., 2024), following the lower uncertainties obtained using other non-asymptotic approaches (Marra et al., 2020). Uncertainties emerging from the Monte Carlo approximation in Eq. (4) can be reduced arbitrarily (in our case they are as small as $\sim 10^{-2}$ mm using N = 20,000). Epistemic uncertainties may arise from the choice of the magnitude model (Marra et al., 2024). Here we used the Weibull distribution, following atmospheric dynamics reasoning (Wilson and Toumi, 2005), empirical evidence (Zorzetto et al., 2016; Marra et al., 2023), and stochastic modeling results (Papalexiou, 2022). Estimation uncertainty for future periods was calculated using the same parameter sets while applying the change of ΔT, $\frac{\sigma_f}{\sigma_p}$, and $\frac{n_f}{n_p}$, as mentioned above.

2.2. The Chicago design storm model

The CDS approach was first introduced by Keifer and Chu (1957). It enables a single synthetic storm to embed a given precipitation return level for all durations of interest based on an intensity–duration curve. In the example presented in Fig. 2, CDS is fit to perfectly simulate rainfall intensities with a prescribed return level (of 100 years in this case) for durations from 10 min (rainfall peak) to 3 h, which is the maximum storm duration of the simulated design storm.

Suppose the intensity–duration curve for a given $\mathcal{T}$-year return level is as follows:

$$I(t_D;\mathcal{T}) = \frac{C_a}{(t_D + C_b)^{C_c}}, \tag{5}$$

where I is the rainfall intensity, t_D is the duration of interest, and C_a, C_b, and C_c are the CDS parameters in the intensity–duration curve.

To determine the three CDS parameters for a given return period $\mathcal{T}$, we minimized the weighted root mean square error (WRMSE) between the observed intensities at the duration of interest $I(t_D,\mathcal{T})$ and the computed ones $\hat{I}_{t_D}$ from the simulated CDS hyetograph:

$$WRMSE = \sqrt{\frac{\Sigma W_{t_D}\left(I_{t_D} - \hat{I}_{t_D}\right)^2}{\Sigma W_{t_D}}}. \tag{6}$$

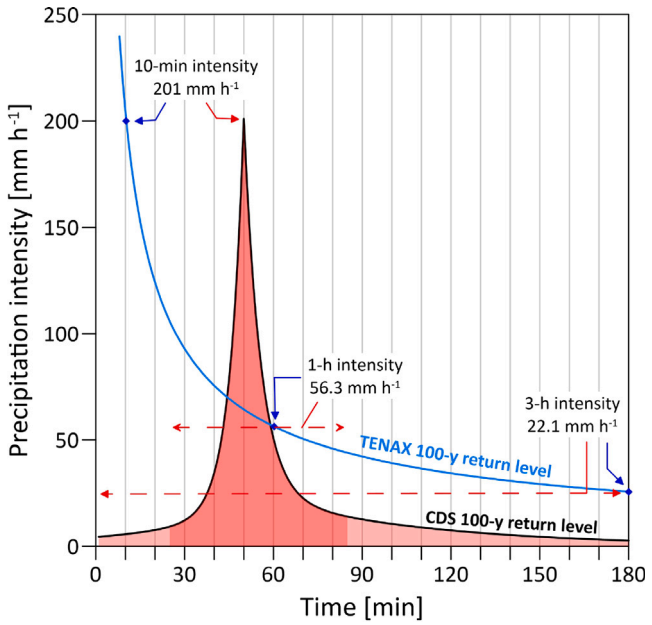

Fig. 2. A hyetograph constructed with the Chicago design storm approach, parameterized to reflect a 100-year return level storm computed from the TENAX model (blue line here and dashed line in Fig. 3). The designed hyetograph is compatible with the rainfall intensity at a 100-year return level of 10 min, and one and three hours.

The weights W_{t_D} computed as:

$$W_{t_D} = \frac{1}{N_{t_D}} \cdot \frac{\Sigma I_{t_D}}{I_{t_D}}, \tag{7}$$

where N_{t_D} is the total number of durations used in the optimization. Weights are required to reduce the effects of higher intensities in the shorter durations, which are much greater than those in the longer durations, and Eq. (7) proposes a weighting method that equalizes this effect.

Then, the CDS hyetograph before the peak can be expressed as:

$$I(t_b; \mathcal{T}) = \frac{C_a\left((1-C_c)(\frac{t_b}{r}) + C_b\right)}{\left(\frac{t_b}{r} + C_b\right)^{C_c+1}}, \tag{8}$$

and after the rainfall peak as:

$$I(t_a; \mathcal{T}) = \frac{C_a\left((1-C_c)(\frac{t_a}{1-r}) + C_b\right)}{\left(\frac{t_a}{1-r} + C_b\right)^{C_c+1}}, \tag{9}$$

where t_a and t_b are the time after and before the rainfall peak (accordingly), and r is the asymmetry of the hyetograph, which defines the point fraction ($0 < r < 1$) within the storm in which the rainfall intensity is at peak.

2.3. The CAflood model

We used the CADDIES/CAFlood 2D cellular automata flood model (Guidolin et al., 2016) to simulate flood inundation maps. It uses a weight-based system and simplified transition rules to replace the shallow water equations to resolve flow movement on a square regular grid (Ghimire et al., 2012; Guidolin et al., 2016), reducing computational expense while ensuring a high level of precision in runoff calculations (Wang et al., 2018). Flow between grid cells is governed by Manning's equation, which takes into account the cells' water surface gradient, surface roughness, and lateral water inflow and outflow from nearby cells. For this purpose, the border between a grid cell and its neighbor is considered a channel with a width equal to the cell length. CAFlood simulates only above-ground runoff; underground piped drainage systems are not modeled directly. To compensate for inflows to such systems, the user can impose an outflow rate to remove runoff from the simulation (Webber et al., 2018). Model inputs consist of time series of uniform or spatially distributed rainfall intensities, as well as static variables such as terrain elevation and surface roughness, whereas model outputs are composed of spatially and temporally variable water depths and flow velocities. The model has been widely used, including in estimating flood impacts using design storms (for some recent examples see: Cao et al. (2020), Vamvakeridou-Lyroudia et al. (2020), Padulano et al. (2021) and Peleg et al. (2022)).

3. Case study

The purpose of this case study is to demonstrate the capabilities and outputs of the TENAX-CDS model. Since we recently investigated how climate change affects extreme rainfall and flooding in Zurich (Switzerland) and its surroundings (Guo et al., 2021; Peleg et al., 2022), we decided to demonstrate the model there.

3.1. Data

A 10-min precipitation and 1-h temperature dataset were acquired for the Zurich Affoltern station (1 km north of Zurich) from MeteoSwiss for the period 1981–2018. The station is part of the SwissMetNet project, which includes approximately 260 automatic stations with a high level of quality control (Landl et al., 2009).

For simplicity, future changes in temperature during wet days (i.e., ΔT and $\frac{\sigma_f}{\sigma_p}$) and the change in the total number of annual rainfall events ($\frac{n_f}{n_p}$), are taken as the values reported for the nearby station Aadorf by Marra et al. (2024). Specifically, for the end of the century (2080–2099) and following the RCP8.5 emission scenario, values of $\Delta T = 2.8$ °C, $\frac{\sigma_f}{\sigma_p} = 0.99$, and $\frac{n_f}{n_p} = 0.93$ were used. These values are the median change in these statistics from 10 regional climate models from the Euro-CORDEX multi-model ensemble, based on the official CH2018 Swiss climate change scenarios (Sørland et al., 2020; Fischer et al., 2022), as further explained in Marra et al. (2024).

For the CAFlood model, we followed the same setup and used the same digital elevation map of 1 m resolution for the city of Zurich as described by Guo et al. (2021).

3.2. Present and future IDF

First, we fitted the TENAX model to compute IDF curves for the present climate for 1- to 100-year return levels and 10 min, 1 h, and 3 h durations (Fig. 3). MeteoSwiss's GEV-based IDF estimates and TENAX's SMEV-based results show good agreement (Fig. 3), with a bias of only 1.7% on average (by comparing the dotted symbols with the blue lines). Similarly, the maximum bias, detected for the 100-y return level and 10-min duration, is only 5.8%, well within the estimation uncertainty. This good fit is in agreement with the ability of the TENAX model to compute IDF curves, as demonstrated for other nearby stations (Marra et al., 2024).

We found the IDF curves for future climates are always higher than those for present climates (Fig. 3). The projected intensification is on average 23.4%, 18.3%, and 16.8% for the 10 min, 1 h, and 3 h durations, respectively. These projected changes are in line with what is expected, with larger changes for shorter durations (Marra et al., 2024).

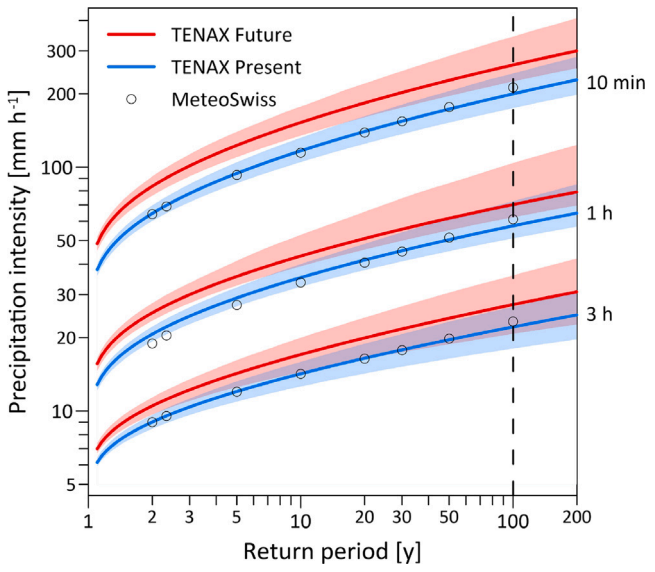

Fig. 3. Intensity–duration–frequency (IDF) curves as computed by the TENAX model for present (1981–2018; blue lines) and future (2080–2099; red lines) climates for 10 min, 1 h, and 3 h duration for the station of Zurich Affoltern. The shaded areas represent the 5–95th range of uncertainty estimated by the TENAX model. The circles represent MeteoSwiss's estimates for the IDF curves; their uncertainties are larger than those from TENAX (not shown, see the comparison in Marra et al. (2024)). The dashed line crosses the 100-y intensity–duration data used to construct the design storm for the present (Figs. 2 and 4) and future (Fig. 4) periods.

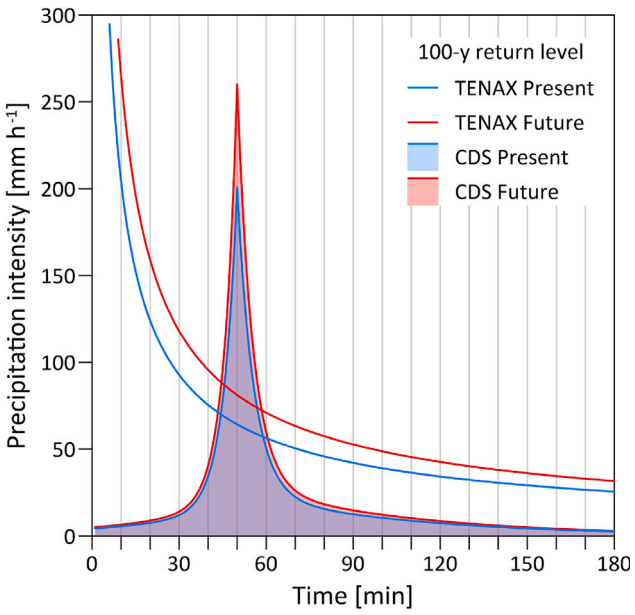

Fig. 4. Intensity–duration curves computed by the TENAX model for present (1981–2018; blue lines) and future (2080–2099; red lines) climates for the 100-year return level, and the CDS hyetographs for present (blue) and future (red).

3.3. Present and future CDS

We then fitted the CDS parameters to the present and future intensity–duration curve at the 100-y return level (Fig. 4). A total storm duration of 3 h was set, with a time resolution of 10 min to match the time resolution of the data, and with an asymmetric r value of 0.3, representing the average time for rainfall to reach its peak in the region (Zeimetz et al., 2018). For the present climate, TENAX intensities are 201 mm h^{-1}, 56.3 mm h^{-1}, and 22.1 mm h^{-1} for the 10 min, 1 h, and 3 h durations respectively. The CDS simulated intensities are identical for the 10 min and 1 h durations, and essentially identical for the 3 h duration (21.07 mm h^{-1}). The same applies when comparing the TENAX and CDS intensities for the future, where TENAX values of 260.2 mm h^{-1} (CDS: 260.2 mm h^{-1}), 70 mm h^{-1} (70 mm h^{-1}), and 27.2 mm h^{-1} (25.9 mm h^{-1}) for the 10 min, 1 h, and 3 h durations, are found in both cases. While near-perfect agreement is observed between the TENAX intensity–duration curves and the CDS with respect to the durations used in the parameter fitting, a bias of up to 10% can be detected for the durations not used in the parameter fitting process. For example, for the 30-min duration, the observed intensity is 105.6 mm h^{-1}, while the CDS intensity is 95.1 mm h^{-1}. It is worth noting that the intensification expected for 10-min intensities (29.5%) is much greater than the one for hourly (24.3%) and three-hour (17.2%) intensities. A quantification of these changes would thus be difficult to achieve even using convection-permitting models as they typically only provide hourly precipitation data, and since these models are unable to resolve orographic convection or shallow convection very well.

3.4. Flood inundation maps

In the final step, we used the CDS time series as inputs to CAFlood. Applying the CDS for the present climate, the average water depth in the city was found to be 0.104 m, while the peak inundation depth in some streets reached over 1 m (Fig. 5a). As a result of the increase in rainfall intensity of about 20% in the future climate (see Section 3.2), the average water depth in the city increased by 14.5% to 0.119 m (Fig. 5b). There are, however, some places where the water depths increase considerably more, sometimes by over 0.5 m (Fig. 5b).

It is worth noting that we use a simple model setup that does not take into account the spatial distribution of land uses and infiltration rates, for example. As such, the flood modeling results obtained should be taken as indicative and not detailed future flood predictions for the city of Zurich.

4. Discussion

In our case study above, we parameterized the TENAX model to generate IDF curves and a CDS for a storm length of 3 h. However, since the temperature–extreme precipitation relation is stable over longer durations, the model can be applied over longer time scales. We have tested the model at the daily duration (not shown) and the relationship still holds, and others have demonstrated that the temperature–precipitation scaling relationship is valid at the daily scale in Switzerland (Scherrer et al., 2016) and elsewhere (Ali et al., 2018). We note that at daily durations and longer, precipitation intermittency may affect the extreme precipitation–temperature relationship (Schleiss, 2018). As such, temperature–precipitation scaling at the daily scale should be evaluated on a case-by-case basis. In addition to this, TENAX's underlying assumption that the magnitude model $W(x;T)$ remains unchanged over time may be less true for durations at daily and longer scales, since extremes may be related to a number of factors (see further discussion in Marra et al. (2024)). Keeping this caveat in mind, the proposed model may be used not only for sub-daily durations, as presented here, but also for longer durations. As a result, the model has the potential to be utilized for a variety of other purposes in addition to the urban flooding demonstrated in our case study. This may be relevant in the context of assessing changes to flash flooding in rural catchments, which may be triggered by longer duration storms, but whose main cause remains convective rainfall over the whole or part of the catchment (Borga et al., 2014).

We used rainfall time series from a single source to represent rainfall falling over the entire city. As such, this simple approach should be revised to incorporate data from several sources and also (if necessary) to account for the differences in scale between the rain gauge (a

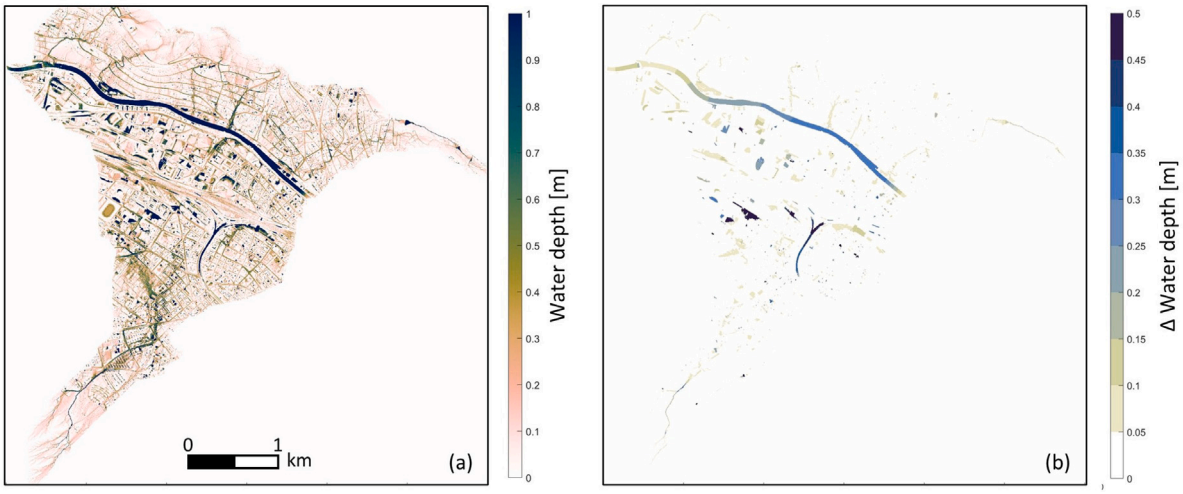

Fig. 5. (a) A simulation of the maximum water depth for Zurich using the 100-year return level CDS for the present climate that is presented in Fig. 4. (b) The difference (future minus present) in simulated water depth for the 100-year return level CDS.

Table 1
Optimizing the CDS for Zurich (Affoltern) station using the official MeteoSwiss (MS) GEV-based intensity estimates for five durations. The results are for the optimization using weights (CDS-WRMSE), and without considering weights (CDS-RMSE).

Duration [min]	MS [mm h^{-1}]	CDS-WRMSE [mm h^{-1}]	CDS-RMSE [mm h^{-1}]
10	212.4	213.7	212.6
30	110.8	106.6	109.2
60	61.1	63	63.3
180	23.3	24.6	22.5
1440	4.5	3.7	2.6

point scale) and the catchment area. It is possible to accomplish the latter by applying an area reduction factor as suggested, for example, by Rosbjerg and Madsen (2019). However, changes in storm spatial structure may require adjustments in the areal reduction factors (Kim et al., 2019).

It has been mentioned previously that the CDS is perfectly matched with the intensity–duration curves for which it has been fitted. In other words, extreme rainfall for different sub-daily durations will all be represented in the synthetic storm; in our case study, the design storm includes simultaneously the peak rainfall intensity for 10 min, 1 h, and 3 h for the 100-y return level (Fig. 2). However, such an extreme rainfall event, in which peak rainfall intensities of different durations for an equivalent recurrence interval are concurrent, is highly unlikely to occur. Therefore, when CDS is applied, it can be expected to simulate the "worst-case scenario" of extreme rainfall and flooding. Furthermore, we currently use the WRMSE (Eq. (6)) as the measure of goodness-of-fit in the CDS parameterization. The minimization process works perfectly well when three durations are considered, as demonstrated in the case study; however, we note that when three or fewer durations are considered, the parameters can be determined analytically without optimization. Using MeteoSwiss intensity–duration estimations for the 100-y return level for the same station, we repeated the optimization with five durations to show that the optimization is also valid for longer durations. As shown in Table 1, the WRMSE minimization works well up to a daily scale, with an average bias of only 6%. If users wish to reduce biases for longer durations, the weights can be adjusted accordingly.

Another point to consider is that the proposed model generates only a single design storm for each intensity–duration curve it is fitted for. As a result, the continuity of rainfall over time is not represented. Consequently, the catchment antecedent conditions prior to the start of the design storm should be estimated independently and set in the hydrological or hydrodynamic model (Watt and Marsalek, 2013). A challenge may arise in this regard, as the catchment antecedent conditions are also expected to be impacted by climate change (Sharma et al., 2021). A hydrodynamic model for an urban catchment, for example, should consider the capacity of the drainage system at the beginning of the simulation of the design storm, whereas in rural catchments, soil saturation conditions and river levels should be taken into consideration.

Equally the shape, or profile, of the design storm, and how this might change with warming, is not taken into consideration in our case study. While in the TENAX-CDS the time to peak and shape of the design storm are defined by r, we used the same $r = 0.3$ value for the present and future climates. Work in the UK by Villalobos Herrera et al. (2023) has shown that real storm profiles can be centered, front-loaded, or back-loaded and this tends to depend on the duration of the storm, with shorter events (1 to 3 h) being predominantly front-loaded and becoming more centered as they become longer in duration. There also appears to be evidence from an observational study in Australia (Visser et al., 2023) that with warmer temperatures, storms become more front-loaded.

As a final point, our case study shows that differences between historical and future IDFs are greater for short durations (i.e., toward 10 min) and for rarer events (Fig. 3). As a matter of fact, at the 100-year return level examined here, the uncertainties in the present and future extreme rainfall intensities are highly overlapping (Fig. 3). This does not imply that at rare recurrence intervals there is no climate change signal, but rather that the estimates are highly uncertain (Fowler et al., 2021). In fact, Marra et al. (2019) demonstrated that using the SMEV approach (embedded in the proposed model, or the TENAX model itself, see Marra et al. (2024)) to estimate IDF, lower uncertainties in the fit can be anticipated in comparison to other common IDF-fit approaches, such as using the GEV method.

We note that the TENAX-CDS model is a more compact version of the TENAX model (Marra et al., 2024; Marra and Peleg, 2023). For example, we have not included the parameter sensitivity estimation or the temperature–precipitation scaling computation in the TENAX-CDS model as in the original TENAX model to make the model lighter and easier to use. However, these features (and others) are present in the original code, which is available open source in Marra and Peleg (2023). Readers are advised to refer to it if they wish to embed them in the CDS version. Moreover, since methods other than CDS are used to estimate flood hazards at different locations, we encourage users to further develop and combine TENAX with alternative approaches based on the provided open-source code.

5. Conclusions

We have presented a new method for computing short-duration IDF curves and design storms for flash flood assessments under increasing temperatures. The physically-based TENAX-CDS model considers both thermodynamical and dynamical changes and is highly efficient in terms of its data requirements and computational costs. It requires a minimal set of parameters and input data, and its projections only rely on simulations of daily temperatures during rainy days from coarse-resolution climate models. An example of its use is provided, as well as the source code for others to use.

Code availability

The TENAX-CDS model is available at https://doi.org/10.5281/zenodo.10491542 (Peleg and Marra, 2024), including the data necessary to reproduce the results for the Zurich (Affoltern) station as an example. Precipitation and temperature data for the Zurich (Affoltern) station in Switzerland shown in the case study is provided by MeteoSwiss and are freely accessible from the IDAWEB at https://gate.meteoswiss.ch/idaweb.

CRediT authorship contribution statement

Nadav Peleg: Writing – review & editing, Writing – original draft, Visualization, Project administration, Methodology, Funding acquisition, Formal analysis, Data curation, Conceptualization. **Daniel B. Wright:** Writing – review & editing, Investigation. **Hayley J. Fowler:** Writing – review & editing, Investigation. **João P. Leitão:** Writing – review & editing, Investigation. **Ashish Sharma:** Writing – review & editing, Investigation. **Francesco Marra:** Writing – review & editing, Writing – original draft, Software, Project administration, Methodology, Funding acquisition, Conceptualization.

Declaration of competing interest

The authors declare that they have no known competing financial interests or personal relationships that could have appeared to influence the work reported in this paper.

Data availability

We shared data and codes (link in the paper)

Acknowledgments

Nadav Peleg was supported by the Swiss National Science Foundation (SNSF), Grant 194649 (“Rainfall and floods in future cities”). Francesco Marra was supported by the Department of Geosciences of the University of Padova (“TENAX” project) as part of the “The Geosciences for Sustainable Development” [CUPC93C23002690001], and by the CARIPARO Foundation through the Excellence Grant 2021 (“Resilience” project). Hayley Fowler was supported by the Climate+ Co-Centre funded by UKRI (NE/Y006496/1) and IMPETUS4CHANGE funded by HORIZON-CL5-2022-D1-02 (Grant agreement ID: 101081555) and the UKRI Horizon Europe Guarantee (10047737).

References

Ali, H., Fowler, H.J., Mishra, V., 2018. Global observational evidence of strong linkage between dew point temperature and precipitation extremes. Geophys. Res. Lett. 45 (22), 12,320–12,330. http://dx.doi.org/10.1029/2018GL080557.

Arnbjerg-Nielsen, K., Willems, P., Olsson, J., Beecham, S., Pathirana, A., Bülow Gregersen, I., Madsen, H., Nguyen, V.-T.-V., 2013. Impacts of climate change on rainfall extremes and urban drainage systems: a review. Water Sci. Technol. 68 (1), 16–28. http://dx.doi.org/10.2166/wst.2013.251.

Balbastre-Soldevila, R., Garcia-Bartual, R., Andres-Domenech, I., 2019. A comparison of design storms for urban drainage system applications. Water 11 (4), http://dx.doi.org/10.3390/w11040757, URL: https://www.mdpi.com/2073-4441/11/4/757.

Berk, M., Špačková, O., Straub, D., 2017. Probabilistic design storm method for improved flood estimation in ungauged catchments. Water Resour. Res. 53 (12), 10701–10722. http://dx.doi.org/10.1002/2017WR020947.

Blanchet, J., Ceresetti, D., Molinié, G., Creutin, J.-D., 2016. A regional GEV scale-invariant framework for intensity–duration–frequency analysis. J. Hydrol. 540, 82–95. http://dx.doi.org/10.1016/j.jhydrol.2016.06.007.

Bordoy, R., Burlando, P., 2014. Stochastic downscaling of precipitation to high-resolution scenarios in orographically complex regions: 1. Model evaluation. Water Resour. Res. 50 (1), 540–561. http://dx.doi.org/10.1002/2012WR013289.

Borga, M., Stoffel, M., Marchi, L., Marra, F., Jakob, M., 2014. Hydrogeomorphic response to extreme rainfall in headwater systems: Flash floods and debris flows. J. Hydrol. 518, 194–205. http://dx.doi.org/10.1016/j.jhydrol.2014.05.022.

Cao, R., Li, F., Feng, P., 2020. Exploring the hydrologic response to the urban building coverage ratio by model simulation. Theor. Appl. Climatol. 140, 1005–1015. http://dx.doi.org/10.1007/s00704-020-03139-x.

Chow, V.T., Maidment, D.R., Mays, L.W., 1988. Applied Hydrology. McGraw-Hill, New York.

Cook, L.M., McGinnis, S., Samaras, C., 2020. The effect of modeling choices on updating intensity-duration-frequency curves and stormwater infrastructure designs for climate change. Clim. Change 159, 289–308. http://dx.doi.org/10.1007/s10584-019-02649-6.

Dinh, T.L.A., Aires, F., 2023. Revisiting the bias correction of climate models for impact studies. Clim. Change 176 (10), 1–30. http://dx.doi.org/10.1007/s10584-023-03597-y.

Fatichi, S., Ivanov, V.Y., Caporali, E., 2011. Simulation of future climate scenarios with a weather generator. Adv. Water Resour. 34 (4), 448–467. http://dx.doi.org/10.1016/j.advwatres.2010.12.013.

Fischer, A., Strassmann, K., Croci-Maspoli, M., Hama, A., Knutti, R., Kotlarski, S., Schär, C., Schnadt Poberaj, C., Ban, N., Bavay, M., Beyerle, U., Bresch, D., Brönnimann, S., Burlando, P., Casanueva, A., Fatichi, S., Feigenwinter, I., Fischer, E., Hirschi, M., Liniger, M., Marty, C., Medhaug, I., Peleg, N., Pickl, M., Raible, C., Rajczak, J., Rössler, O., Scherrer, S., Schwierz, C., Seneviratne, S., Skelton, M., Sørland, S., Spirig, C., Tschurr, F., Zeder, J., Zubler, E., 2022. Climate scenarios for Switzerland CH2018 - approach and implications. Clim. Serv. 26, 100288. http://dx.doi.org/10.1016/j.cliser.2022.100288.

Fowler, H.J., Lenderink, G., Prein, A.F., Westra, S., Allan, R.P., Ban, N., Barbero, R., Berg, P., Blenkinsop, S., Do, H.X., et al., 2021. Anthropogenic intensification of short-duration rainfall extremes. Nat. Rev. Earth Environ. 2 (2), 107–122. http://dx.doi.org/10.1038/s43017-020-00128-6.

Ghimire, B., Chen, A.S., Guidolin, M., Keedwell, E.C., Djordjević, S., Savić, D.A., 2012. Formulation of a fast 2D urban pluvial flood model using a cellular automata approach. J. Hydroinform. 15 (3), 676–686. http://dx.doi.org/10.2166/hydro.2012.245.

Guidolin, M., Chen, A.S., Ghimire, B., Keedwell, E.C., Djordjević, S., Savić, D.A., 2016. A weighted cellular automata 2D inundation model for rapid flood analysis. Environ. Model. Softw. 84, 378–394. http://dx.doi.org/10.1016/j.envsoft.2016.07.008.

Guo, Z., Leitão, J.P., Simões, N.E., Moosavi, V., 2021. Data-driven flood emulation: Speeding up urban flood predictions by deep convolutional neural networks. J. Flood Risk Manag. 14 (1), e12684. http://dx.doi.org/10.1111/jfr3.12684.

Hicks, W.I., 1944. A method of computing urban runoff. Trans. Am. Soc. Civ. Eng. 109 (1), 1217–1253. http://dx.doi.org/10.1061/TACEAT.0005713, URL: https://ascelibrary.org/doi/abs/10.1061/TACEAT.0005713.

Innocenti, S., Mailhot, A., Frigon, A., 2017. Simple scaling of extreme precipitation in north america. Hydrol. Earth Syst. Sci. 21 (11), 5823–5846. http://dx.doi.org/10.5194/hess-21-5823-2017.

Keifer, C.J., Chu, H.H., 1957. Synthetic storm pattern for drainage design. J. Hydraul. Div. 83 (4), 1332–1–1332–25. http://dx.doi.org/10.1061/JYCEAJ.0000104, URL: https://ascelibrary.org/doi/abs/10.1061/JYCEAJ.0000104.

Kilsby, C., Jones, P., Burton, A., Ford, A., Fowler, H., Harpham, C., James, P., Smith, A., Wilby, R., 2007. A daily weather generator for use in climate change studies. Environ. Model. Softw. 22 (12), 1705–1719. http://dx.doi.org/10.1016/j.envsoft.2007.02.005.

Kim, J., Lee, J., Kim, D., Kang, B., 2019. The role of rainfall spatial variability in estimating areal reduction factors. J. Hydrol. 568, 416–426. http://dx.doi.org/10.1016/j.jhydrol.2018.11.014.

Kuichling, E., 1889. The relation between the rainfall and the discharge of sewers in populous districts. Trans. Am. Soc. Civ. Eng. 20 (1), 1–56.

Kundzewicz, Z.W., Kanae, S., Seneviratne, S.I., Handmer, J., Nicholls, N., Peduzzi, P., Mechler, R., Bouwer, L.M., Arnell, N., Mach, K., et al., 2014. Flood risk and climate change: global and regional perspectives. Hydrol. Sci. J. 59 (1), 1–28. http://dx.doi.org/10.1080/02626667.2013.857411.

Landl, B., Roulet, Y.-A., Calpini, B., 2009. SwissMetNet: operational quality control on raw data of the new automatic meteorological ground-based network of Switzerland. In: 9th EMS Annual Meeting. pp. EMS2009–453.

Lima, C.H., Kwon, H.-H., Kim, Y.-T., 2018. A local-regional scaling-invariant Bayesian GEV model for estimating rainfall IDF curves in a future climate. J. Hydrol. 566, 73–88. http://dx.doi.org/10.1016/j.jhydrol.2018.08.075.

Madsen, H., Lawrence, D., Lang, M., Martinkova, M., Kjeldsen, T., 2014. Review of trend analysis and climate change projections of extreme precipitation and floods in europe. J. Hydrol. 519, 3634–3650. http://dx.doi.org/10.1016/j.jhydrol.2014.11.003.

Maimone, M., Malter, S., Anbessie, T., Rockwell, J., 2023. Three methods of characterizing climate-induced changes in extreme rainfall: a comparison study. J. Water Clim. Change 14 (11), 4245–4260. http://dx.doi.org/10.2166/wcc.2023.420.

Marani, M., Ignaccolo, M., 2015. A metastatistical approach to rainfall extremes. Adv. Water Resour. 79, 121–126. http://dx.doi.org/10.1016/j.advwatres.2015.03.001.

Markolf, S.A., Chester, M.V., Helmrich, A.M., Shannon, K., 2021. Re-imagining design storm criteria for the challenges of the 21st century. Cities 109, 102981. http://dx.doi.org/10.1016/j.cities.2020.102981.

Marra, F., Amponsah, W., Papalexiou, S.M., 2023. Non-asymptotic Weibull tails explain the statistics of extreme daily precipitation. Adv. Water Resour. 173, 104388. http://dx.doi.org/10.1016/j.advwatres.2023.104388.

Marra, F., Borga, M., Morin, E., 2020. A unified framework for extreme subdaily precipitation frequency analyses based on ordinary events. Geophys. Res. Lett. 47 (18), e2020GL090209. http://dx.doi.org/10.1029/2020GL090209.

Marra, F., Koukoula, M., Canale, A., Peleg, N., 2024. Predicting extreme sub-hourly precipitation intensification based on temperature shifts. Hydrol. Earth Syst. Sci. 28 (2), 375–389. http://dx.doi.org/10.5194/hess-28-375-2024.

Marra, F., Peleg, N., 2023. Temperature-Dependent Non-Asymptotic Statistical Model for Extreme Return Levels. TENAX, Zenodo, http://dx.doi.org/10.5281/zenodo.8345905.

Marra, F., Zoccatelli, D., Armon, M., Morin, E., 2019. A simplified MEV formulation to model extremes emerging from multiple nonstationary underlying processes. Adv. Water Resour. 127, 280–290. http://dx.doi.org/10.1016/j.advwatres.2019.04.002.

Marsalek, J., Watt, W.E., 1984. Design storms for urban drainage design. Can. J. Civil Eng. 11 (3), 574–584. http://dx.doi.org/10.1139/l84-075.

Martel, J.-L., Brissette, F.P., Lucas-Picher, P., Troin, M., Arsenault, R., 2021. Climate change and rainfall intensity–duration–frequency curves: Overview of science and guidelines for adaptation. J. Hydrol. Eng. 26 (10), 03121001. http://dx.doi.org/10.1061/(ASCE)HE.1943-5584.0002122.

Min, S.-K., Zhang, X., Zwiers, F.W., Hegerl, G.C., 2011. Human contribution to more-intense precipitation extremes. Nature 470 (7334), 378–381. http://dx.doi.org/10.1038/nature09763.

Moraga, J.S., Peleg, N., Fatichi, S., Molnar, P., Burlando, P., 2021. Revealing the impacts of climate change on mountainous catchments through high-resolution modelling. J. Hydrol. 603, 126806. http://dx.doi.org/10.1016/j.jhydrol.2021.126806.

Ochoa-Rodriguez, S., Wang, L.-P., Gires, A., Pina, R.D., Reinoso-Rondinel, R., Bruni, G., Ichiba, A., Gaitan, S., Cristiano, E., van Assel, J., Kroll, S., Murlà-Tuyls, D., Tisserand, B., Schertzer, D., Tchiguirinskaia, I., Onof, C., Willems, P., ten Veldhuis, M.-C., 2015. Impact of spatial and temporal resolution of rainfall inputs on urban hydrodynamic modelling outputs: A multi-catchment investigation. J. Hydrol. 531, 389–407. http://dx.doi.org/10.1016/j.jhydrol.2015.05.035.

Padulano, R., Rianna, G., Costabile, P., Costanzo, C., Del Giudice, G., Mercogliano, P., 2021. Propagation of variability in climate projections within urban flood modelling: A multi-purpose impact analysis. J. Hydrol. 602, 126756. http://dx.doi.org/10.1016/j.jhydrol.2021.126756.

Papalexiou, S.M., 2022. Rainfall generation revisited: Introducing CoSMoS-2s and advancing copula-based intermittent time series modeling. Water Resour. Res. 58 (6), e2021WR031641. http://dx.doi.org/10.1029/2021WR031641.

Peleg, N., Ban, N., Gibson, M.J., Chen, A.S., Paschalis, A., Burlando, P., Leitao, J.P., 2022. Mapping storm spatial profiles for flood impact assessments. Adv. Water Resour. 166, 104258. http://dx.doi.org/10.1016/j.advwatres.2022.104258.

Peleg, N., Blumensaat, F., Molnar, P., Fatichi, S., Burlando, P., 2017. Partitioning the impacts of spatial and climatological rainfall variability in urban drainage modeling. Hydrol. Earth Syst. Sci. 21 (3), 1559–1572. http://dx.doi.org/10.5194/hess-21-1559-2017.

Peleg, N., Marra, F., 2024. He TENAX-CDS Model: A Simple Approach for Adapting Design Storms to Assess Climate-Induced Changes in Flash Flood Risk. Zenodo, http://dx.doi.org/10.5281/zenodo.10491542.

Peleg, N., Molnar, P., Burlando, P., Fatichi, S., 2019. Exploring stochastic climate uncertainty in space and time using a gridded hourly weather generator. J. Hydrol. 571, 627–641. http://dx.doi.org/10.1016/j.jhydrol.2019.02.010.

Prein, A.F., Langhans, W., Fosser, G., Ferrone, A., Ban, N., Goergen, K., Keller, M., Tölle, M., Gutjahr, O., Feser, F., Brisson, E., Kollet, S., Schmidli, J., van Lipzig, N.P.M., Leung, R., 2015. A review on regional convection-permitting climate modeling: Demonstrations, prospects, and challenges. Rev. Geophys. 53 (2), 323–361. http://dx.doi.org/10.1002/2014RG000475.

Prein, A.F., Rasmussen, R.M., Ikeda, K., Liu, C., Clark, M.P., Holland, G.J., 2017. The future intensification of hourly precipitation extremes. Nat. Clim. Change 7 (1), 48–52. http://dx.doi.org/10.1038/nclimate3168.

Rajulapati, C.R., Papalexiou, S.M., 2023. Precipitation bias correction: A novel semi-parametric quantile mapping method. Earth Space Sci. 10 (4), e2023EA002823. http://dx.doi.org/10.1029/2023EA002823.

Rosbjerg, D., Madsen, H., 2019. Initial design of urban drainage systems for extreme rainfall events using intensity-duration-area (IDA) curves and chicago design storms (CDS). Hydrol. Sci. J. 64 (12), 1397–1403. http://dx.doi.org/10.1080/02626667.2019.1645958.

Rosenzweig, B.R., McPhillips, L., Chang, H., Cheng, C., Welty, C., Matsler, M., Iwaniec, D., Davidson, C.I., 2018. Pluvial flood risk and opportunities for resilience. WIREs Water 5 (6), e1302. http://dx.doi.org/10.1002/wat2.1302.

Scherrer, S.C., Fischer, E.M., Posselt, R., Liniger, M.A., Croci-Maspoli, M., Knutti, R., 2016. Emerging trends in heavy precipitation and hot temperature extremes in Switzerland. J. Geophys. Res.: Atmos. 121 (6), 2626–2637. http://dx.doi.org/10.1002/2015JD024634.

Schlef, K.E., Kunkel, K.E., Brown, C., Demissie, Y., Lettenmaier, D.P., Wagner, A., Wigmosta, M.S., Karl, T.R., Easterling, D.R., Wang, K.J., et al., 2023. Incorporating non-stationarity from climate change into rainfall frequency and intensity-duration-frequency (IDF) curves. J. Hydrol. 616, 128757. http://dx.doi.org/10.1016/j.jhydrol.2022.128757.

Schleiss, M., 2018. How intermittency affects the rate at which rainfall extremes respond to changes in temperature. Earth Syst. Dyn. 9 (3), 955–968. http://dx.doi.org/10.5194/esd-9-955-2018.

Sharma, A., Hettiarachchi, S., Wasko, C., 2021. Estimating design hydrologic extremes in a warming climate: alternatives, uncertainties and the way forward. Phil. Trans. R. Soc. A 379 (2195), 20190623. http://dx.doi.org/10.1098/rsta.2019.0623.

Smith, A., Bates, P., Freer, J., Wetterhall, F., 2014. Investigating the application of climate models in flood projection across the UK. Hydrol. Process. 28 (5), 2810–2823. http://dx.doi.org/10.1002/hyp.9815.

Sørland, S.L., Fischer, A.M., Kotlarski, S., Künsch, H.R., Liniger, M.A., Rajczak, J., Schär, C., Spirig, C., Strassmann, K., Knutti, R., 2020. CH2018 - national climate scenarios for Switzerland: How to construct consistent multi-model projections from ensembles of opportunity. Clim. Serv. 20, 100196. http://dx.doi.org/10.1016/j.cliser.2020.100196.

Tholin, A.L., Keifer, C.J., 1960. Hydrology of urban runoff. Trans. Am. Soc. Civ. Eng. 125 (1), 1308–1355. http://dx.doi.org/10.1061/TACEAT.0007893, URL: https://ascelibrary.org/doi/abs/10.1061/TACEAT.0007893.

Trenberth, K.E., Dai, A., Rasmussen, R.M., Parsons, D.B., 2003. The changing character of precipitation. Bull. Am. Meteorol. Soc. 84 (9), 1205–1218. http://dx.doi.org/10.1175/BAMS-84-9-1205.

Vamvakeridou-Lyroudia, L., Chen, A., Khoury, M., Gibson, M., Kostaridis, A., Stewart, D., Wood, M., Djordjevic, S., Savic, D., 2020. Assessing and visualising hazard impacts to enhance the resilience of critical infrastructures to urban flooding. Sci. Total Environ. 707, 136078. http://dx.doi.org/10.1016/j.scitotenv.2019.136078.

Villalobos Herrera, R., Blenkinsop, S., Guerreiro, S.B., Dale, M., Faulkner, D., Fowler, H.J., 2023. Towards new design rainfall profiles for the United Kingdom. J. Flood Risk Manag. e12958. http://dx.doi.org/10.1111/jfr3.12958.

Visser, J.B., Wasko, C., Sharma, A., Nathan, R., 2023. Changing storm temporal patterns with increasing temperatures across Australia. J. Clim. 36 (18), 6247–6259. http://dx.doi.org/10.1175/JCLI-D-22-0694.1.

Wang, Y., Chen, A.S., Fu, G., Djordjević, S., Zhang, C., Savić, D.A., 2018. An integrated framework for high-resolution urban flood modelling considering multiple information sources and urban features. Environ. Model. Softw. 107, 85–95. http://dx.doi.org/10.1016/j.envsoft.2018.06.010.

Wang, A.K., Dominguez, F., Schmidt, A.R., 2019. Extreme precipitation spatial analog: In search of an alternative approach for future extreme precipitation in urban hydrological studies. Water 11 (5), http://dx.doi.org/10.3390/w11051032.

Watt, E., Marsalek, J., 2013. Critical review of the evolution of the design storm event concept. Can. J. Civil Eng. 40 (2), 105–113. http://dx.doi.org/10.1139/cjce-2011-0594.

Webber, J., Gibson, M., Chen, A., Savic, D., Fu, G., Butler, D., 2018. Rapid assessment of surface-water flood-management options in urban catchments. Urb. Water J. 15 (3), 210–217. http://dx.doi.org/10.1080/1573062X.2018.1424212.

Willems, P., Arnbjerg-Nielsen, K., Olsson, J., Nguyen, V., 2012. Climate change impact assessment on urban rainfall extremes and urban drainage: Methods and shortcomings. Atmos. Res. 103, 106–118. http://dx.doi.org/10.1016/j.atmosres.2011.04.003.

Wilson, P., Toumi, R., 2005. A fundamental probability distribution for heavy rainfall. Geophys. Res. Lett. 32 (14), http://dx.doi.org/10.1029/2005GL022465.

Wright, D.B., Yu, G., England, J.F., 2020. Six decades of rainfall and flood frequency analysis using stochastic storm transposition: Review, progress, and prospects. J. Hydrol. 585, 124816. http://dx.doi.org/10.1016/j.jhydrol.2020.124816.

Yin, J., Gentine, P., Zhou, S., Sullivan, S.C., Wang, R., Zhang, Y., Guo, S., 2018. Large increase in global storm runoff extremes driven by climate and anthropogenic changes. Nat. Commun. 9 (1), 4389. http://dx.doi.org/10.1038/s41467-018-06765-2.

Yu, G., Wright, D.B., Li, Z., 2020. The upper tail of precipitation in convection-permitting regional climate models and their utility in nonstationary rainfall and flood frequency analysis. Earth's Future 8 (10), e2020EF001613. http://dx.doi.org/10.1029/2020EF001613.

Zeimetz, F., Schaefli, B., Artigue, G., Hernández, J.G., Schleiss, A.J., 2018. Swiss rainfall mass curves and their influence on extreme flood simulation. Water Resour. Manag. 32, 2625–2638. http://dx.doi.org/10.1007/s11269-018-1948-y.

Zorzetto, E., Botter, G., Marani, M., 2016. On the emergence of rainfall extremes from ordinary events. Geophys. Res. Lett. 43 (15), 8076–8082. http://dx.doi.org/10.1002/2016GL069445.